MRS Advances © 2016 Materials Research Society
DOI: 10.1557/adv.2016.510

$Al_{1-x}Sc_xN$ Thin Film Structures for Pyroelectric Sensing Applications

V. Vasilyev, J. Cetnar, B. Claflin, G. Grzybowski, K. Leedy, N. Limberopoulos, D. Look, and S. Tetlak

Air Force Research Laboratory, Wright-Patterson AFB, Dayton, OH

ABSTRACT

AlN thin film structures have many useful and practical piezoelectric and pyroelectric properties. The potential enhancement of the AlN piezo- and pyroelectric constants allows it to compete with more commonly used materials. For example, combination of AlN with ScN leads to new structural, electronic, and mechanical characteristics, which have been reported to substantially enhance the piezoelectric coefficients in solid-solution AlN-ScN compounds, compared to a pure AlN-phase material.

In our work, we demonstrate that an analogous alloying approach results in considerable enhancement of the pyroelectric properties of AlN - ScN composites. Thin films of ScN, AlN and $Al_{1-x}Sc_xN$ (x = 0 – 1.0) were deposited on silicon (004) substrates using dual reactive sputtering in Ar/N_2 atmosphere from Sc and Al targets. The deposited films were studied and compared using x-ray diffraction, XPS, SEM, and pyroelectric characterization. An up to 25% enhancement was observed in the pyroelectric coefficient (Pc = 0.9 μC /m^{2}K) for $Sc_{1-x}Al_xN$ thin films structures in comparison to pure AlN thin films (Pc = 0.71 μC/m^{2}K). The obtained results suggest that $Al_{1-x}Sc_xN$ films could be a promising novel pyroelectric material and might be suitable for use in uncooled IR detectors.

INTRODUCTION

Wurtzite-type AlN and GaN thin films and AlGaN structures are currently extensively studied due to their great performance in contemporary electronics, including highly efficient LEDs, energy harvesting, and other multifunctional devices [1]. One of the most challenging and serious problems is a requirement for highly sensitive and affordable uncooled detectors in the visible and infrared (IR) wavelength ranges. Development and implementation of novel pyroelectric (PE) materials with enhanced sensing capabilities would be an effective solution for such detectors. Since AlN thin film structures have reasonable PE properties, there are growing applications in this area [2 – 6]. The potential further enhancement of the AlN PE constants would allow AlN to compete with more commonly used materials.

AlN's PE coefficient P_c is small relative to those seen in ferroelectric oxide films. Nonetheless, AlN presents a PE figure of merit F_D near the same magnitude as typically used PE materials [5]. Its overall PE properties are still attractive due to the relatively small dielectric constant ε_r and low dielectric losses $tan\delta$. It is also important to note that processing of AlN thin film structures is well developed in comparison to ferroelectric pyroelectrics and is compatible with contemporary CMOS technology [7]. Therefore, any success in research efforts that leads to the enhancement of AlN sensing capabilities would increase the chances of AlN to be a suitable material for use in uncooled PE IR detectors.

One of the methods of improving AlN's PE performance is to form AlN alloys with rock-salt structure transition-metal nitrides, like ScN, TiN, and CrN. For example, the combination of

AlN with ScN leads to new structural, electronic, and mechanical characteristics, which have been reported in [8] to substantially enhance (~400%) the piezoelectric coefficient $\boldsymbol{d_{33}}$ in solid-solution compounds, such as $Al_{0.57}Sc_{0.43}N$ compared to pure AlN-phase material..

If the new AlN – ScN alloy retains the same wurtzite structure type, it is possible that a significant increase of the total PE effect, which consists of primary and secondary part, where the piezoelectric component brings a significant input [9]. The published data [8, 10] make it clear that the observed enhancement of piezoelectric properties in $\mathbf{Al_{1-x}}Sc_xN$ is an intrinsic effect and is due to the reorganization of the wurtzite structure in which the Sc concentration increases, thus changing the cell parameter ratio *c/a*. Consequently, the similar alloying approach, which was used for piezoelectric enhancement, may result in considerable improvement of the PE properties of $\mathbf{Al_{1-x}}Sc_xN$ solid solutions. In our work we evaluate first only the total PE effect.

EXPERIMENT

$\mathbf{Al_{1-x}}Sc_xN$ (x = 0 – 1.0) thin films were deposited in a Kurt J. Lesker Lab 18 load-locked sputtering system on 3-inch n-type single-side polished Si (004) wafers by dual reactive magnetron sputtering from two metal Al (99.999%) and Sc (99.99%) targets (pulsed DC power and RF sources, respectively). The substrate temperature was kept constant at 400°C in all deposition experiments. The chamber base pressure was ~3 $x10^{-8}$ Torr. Procedures were followed to minimize residual moisture and oxygen in the chamber including 500°C pre-deposition annealing, 10 min sputter cleaning, and extended process gas purging. The flow rate of the 60%/40% Ar/N_2 reactive gas mixture combined with a throttled high vacuum valve yielded a deposition pressure of 5.2 mTorr. The sputtering rate of Al and Sc ions in plasma was regulated by variation of power applied for each source. While power applied to the Sc target was kept constant at 250W, the power on the Al target varied in a range of 75 to 200 W. The pulse power supply operated at 75 kHz with a 1 μsec reverse time. Finally, the deposition rate of the film was 2 to 4 nm/min. Spectroscopic ellipsometry measurements with a Horiba Jobin Yvon UVISEL were performed to determine the thickness of the deposited films.

X-ray diffraction analysis was performed using a PANalytical X-Pert diffractometer with a hybrid monochromator for Cu $K\alpha_1$ radiation (λ=1.5406Å). The symmetrical ω-2Θ scan method was used to define out-of-plane diffraction peaks and calculate the lattice constants. The ω – rocking curve scans were acquired to determine crystalline quality. We used a polycrystalline ceramic of AlN (99.99%) to determine the unstrained lattice constants c_0 =4.975 Å and a_0 = 3.1096 Å in wurtzite structure (compare with c_0 =4.978 Å and a_0 = 3.111 Å in [11]).

Atomic compositions of films were determined by x-ray photoelectron spectroscopy (XPS) using a PHI (Perkin-Elmer) 5500 spectrometer equipped with a hemispherical analyzer and a Mg Kα x-ray source operated at 350 W. High-resolution spectra of Sc *2p3/2*, O *1s*, N *1s*, and Al *2p* photoelectron peaks were acquired at a pass energy of 58.7eV through a 1.6 mm^2 aperture. Depth profiles were acquired using an Ar ion sputtering source operated at 5 keV, at a sputtering rate of 1.5 nm⁄min. For these depth profiles, atomic concentrations were determined following each sputter treatment from integrated core-level XPS peaks using known sensitivity factors [12].

A Hitachi SU70 Scanning Electron Microscope was employed to acquire the morphology images of deposited $\mathbf{Sc_xAl_{1-x}}N$ films.

To determine both the PE current I_p and PE coefficient P_c in deposited $\mathbf{Al_{1-x}}Sc_xN$ films, a system based on the dynamic capacitance measurements [13], as described in [5], was used in this work. The apparatus exploits thermoelectric heating and cooling both to stabilize and

modulate sample temperature for stimulating the sample PE current. The P_c testing specimen was usually a capacitor, consisting of a thin film of $Al_{1-x}Sc_xN$ deposited on low resistance Si substrate (a bottom electrode, 300 μm thickn.). A 10 – 30 nm NiCr thin film deposited on the $Al_{1-x}Sc_xN$ surface served as the top contact (1cm dia.). Equation (1) from [2, 5] was then used to calculate the PE coefficient:

$$P_c = \left(\frac{I_p}{A \cdot dT/dt}\right) \quad (1)$$

where I_p = PE current, A = specimen's surface area, dT/dt = temperature modulation.

DISCUSSION

The properties of processed thin films are summarized in Table I. According to the XPS analysis, all deposited $Al_{1-x}Sc_xN$ films are nearly stoichiometric with the (Al+Sc)/N ratio being close to 1 and with Sc and Al being constant throughout the film with an accuracy of ~5%. All

Table I. Crystalline properties and PE coefficients in $Al_{1-x}Sc_xN$ (x = 0 – 1).

Property	Stoichiometry						
	AlN	**$Al_{0.8}Sc_{0.2}N$**	**$Al_{0.6}Sc_{0.4}N$**	**$Al_{0.5}Sc_{0.5}N$**	**$Al_{0.4}Sc_{0.6}N$**	**$Al_{0.3}Sc_{0.7}N$**	**ScN**
Oxygen (at. %)	14	12	10	11	17	18	<20
Structure	Wurtzite	Wurtzite	Wurtzite	Wurtzite	Wurtzite	Wurtzite	Rock Salt
Phase Impurity				R.S. ~ 3%	R.S. ~ 4%	R.S. ~ 5%	
Wurtzite, *c* (Å)	4.987	4.991	4.993	5.026	5.067	5.046	
(002) FWHM, deg.	0.464	0.529	0.839	0.215	0.249	0.239	
Wurtzite, *a* (Å)	3.115	N/A	3.135	3.085	3.113	3.102	
c / *a*	1.601	N/A	1.592	1.629	1.628	1.627	
c - strain	0.25	0.32	0.32	1.03	1.86	1.43	
Thickness, nm	370	290	300	225	210	215	190
Rock Salt, *a* (Å)				4.399	4.416	4.469	4.507
(002) FWHM, deg.				1.032	0.668	1.736	0.713
*P*c (μC/m^{2}K)	0.71	0.72	0.73	0.9	0.87	0.86	

specimens contain a similar concentration of oxygen (average 14 at. %) of throughout the film. An increase in oxygen concentration closer to the Si substrate surface and at the top film surface is most likely due to the presence of a native SiO_2 on the Si substrates and some oxygen absorption on the grains of the textured film from exposure of the films to air, respectively. A typical plot of an XPS profile for the $Sc_{0.5}Al_{0.5}N$ film is shown in Fig. 1.

X-ray diffraction analysis revealed the presence of an $Al_{1-x}Sc_xN$ solid solution phase of wurtzite type structure for specimens throughout x = 0 – 0.7. Diffractograms of these specimens show a polycrystalline character of films with typical (002), (101), (102), (110), and (004) reflections for AlN [5]. For specimens with x = 0 – 0.4, values of *c* and *a* cell constants are consistent with the constants for pure AlN phase. A calculated strain along the *c* axis from the ratio $[(c–c_0)/c_0]*100$, where c_0 is the cell constant of unstrained AlN (see our data above), showed the modest values of 0.25-0.32%. For $Al_{1-x}Sc_xN$ specimens with x = 0.5 – 0.7, a considerable increment of the lattice constant *c*, *c* – strain value, and *c*/*a* ratio were observed. This is probably due to the process of incorporation into AlN wurtzite cell of another type of phase, based on layered hexagonal *h*-ScN structure, as described in [10]. This phase appeared

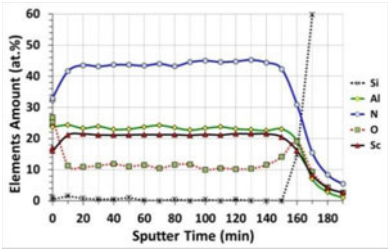

Figure 1. XPS depth profile from the $Al_{0.5}Sc_{0.5}N$ film deposited on Si wafer at 400°C.

to be unstable in the wurtzite configuration, but is more stable as a layered hexagonal cell with $c/a \approx 1.20$. The increase of concentration of incorporated *h*-ScN phase with substantially different *c*, *a* and *c*/*a* parameters causes significant transformation of the dominant wurtzite phase structure and substantially alters the physical properties of $Al_{1-x}Sc_xN$. For example, it leads to considerable increase of the piezoelectric constant d_{33} in $Al_{1-x}Sc_xN$ [6].

As one can see from the Table, the dramatic structural changes can only be seen in $Al_{1-x}Sc_xN$ for samples with x = 0.5 – 0.7. The increase of wurtzite *c*-parameter from 4.987 to 5.067Å (~1.6%) for this Sc-concentration range in $Al_{1-x}Sc_xN$ is consistent with the data predicted and calculated in [14]. The *a*-parameter does not show direct correlation with changes in x, but an elevated (~1.7%) *c*/*a* ratio was found to be equal 1.628 in comparison to 1.599 for unstrained AlN, and it exhibited stability for x = 0.5 – 0.7.

A small amount (~3–5 wt.%) of impure rock-salt type phase for specimens with x = 0.5 – 0.7 was also observed. This fact is supported by appearance in x-ray diffraction scans of low intensity peaks positioned around $2\Theta \sim 40^o$ (Fig. 2a), which we ascribed to (002) reflection peaks in the rock-salt structure [15]. This is consistent with [8] separation of wurtzite and rock-salt phases with the increase in ScN concentration in $Al_{1-x}Sc_xN$ with x = 0.5 – 1.0. Fig. 2b shows a

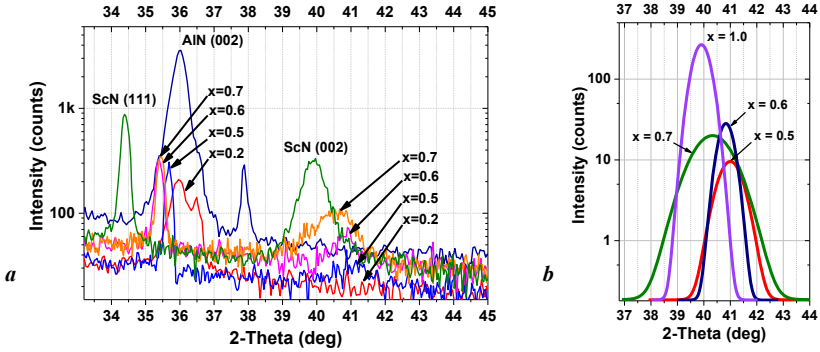

Figure 2. XRD plots (a) for $Al_{1-x}Sc_xN$ (x = 0.2 – 0.7) films in comparison to AlN and ScN pure phase films and (b) Gaussian fitted plots of out-of-plane x-ray scans for (002) reflection of impure polycrystalline phase of $Al_{1-x}Sc_xN$ (x = 0.5 – 1.0) with rock-salt structure.

comparison of the Gaussian fitted plots of the x-ray diffraction scans for these peaks. Additionally, when compared to the data in Table I, one can see that the increase of the AlN concentration in solid solution of $Al_{1-x}Sc_xN$ rock-salt structure leads to an increase in the *a*- cell constant (which is in a good agreement with [16]) due to substitution of rock-salt AlN with much smaller *a*-constant (reported as 4.045Å in [17]) in comparison to 4.507 Å (our data) for ScN. All of the (002) rock-salt peaks shown are rather diffuse and their FWHMs may be evidence of their reduced stability. These might be considered as structural and electronic defects that lead, in turn, to deterioration of the basic PE or piezoelectric properties. The SEM image in Fig. 3 (a) is evidence of presence of two different phase morphologies in $Al_{0.3}Sc_{0.7}N$. One can see the inclusions of micro-crystallites (which very likely might be a rock-salt phase) into the dominant columnar structure (wurtzite) phase. In Fig. 4 (b) a SEM image of pure ScN rock-salt phase with preferable (111) plane and the presence of (002) plane reflection is shown.

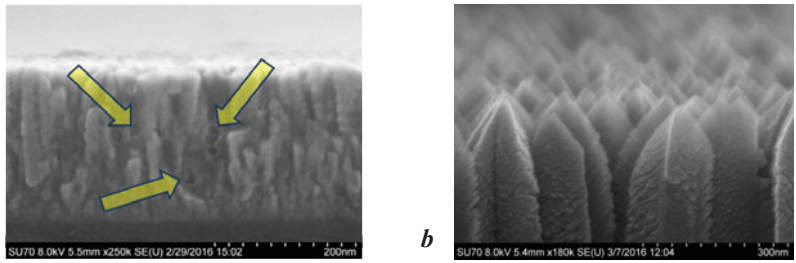

Figure 3. SEM images of (a) the $Al_{0.3}Sc_{0.7}N$ film with the presence of inclusions of rock-salt phase micro-crystallites into wurtzite columnar phase, and (b) rock-salt ScN film with preferable (111) orientation and the presence of (002) plane reflection.

As mentioned above, all of the $Al_{1-x}Sc_xN$ specimens are polycrystalline with preferred crystalline orientation in dominant phases: (002) for wurtzite type (x = 0 – 0.7), and (111) for rock-salt type ScN (x = 1.0). In the case of textured AlN polycrystalline films, large PE coefficients have been measured [3–5], which were apparently due to unique surface phenomena, like energy bending at grain boundaries. In this work, while performing measurements of PE coefficient *Pc* with 1Hz temperature modulation, we determined *Pc* for $Al_{1-x}Sc_xN$ (x = 0.5 – 0.7) specimens with up to 25% enhancement relative to pure AlN film as seen in Table I. Such augmentation is in direct correlation with transformation of the structural parameters of a wurtzite type cell, namely, due to increase of *c*/*a* ratio, which may lead to increased electrical polarization of Al–N bond dipole moment in the wurtzite structure. An enlargement of the *c*-strain, which can affect the PE response, is a result of the interaction between film strain, crystal orientation of various grains and grain sizes. As one can see from Table I, the specimens with elevated *Pc* have reduced value of (002) FWHM data relatively to specimens with lower ScN concentration. This might be associated with the larger grain sizes. In line with further engineering the *c*/*a* ratio, this might be another way to increase PE properties of $Al_{1-x}Sc_xN$ thin films – growth of films with smaller grains that provides a larger ratio surface area to film volume [18]. With a large volume of the film being comprised of grain boundaries, where energy bending is prevalent, this can significantly affect the PE response. It is important to note that a

sizeable amount of oxygen was observed in our samples. Oxygen ions may fill nitrogen vacancies in the coordination tetrahedrons AlN4 and NAl4 of the nitrogen sub-lattice of non-stoichiometric wurtzite AlN [19]. This process may cause significant deformation of local symmetry in these tetrahedrons and also form a new polar V_{Al}^{-3}–$3O_N^{+1}$ complex with the dipole moment that can contribute to the PE effect.

Consideration of all factors leading to the increase or decrease of electrical polarization in wurtzite structure is a non-trivial task due to the exceptional complexity of the PE phenomenon [20]. A more detailed and in-depth study of structural and phase correlations with PE and piezoelectric properties of $Al_{1-x}Sc_xN$ compositions will be a goal of future work.

CONCLUSIONS

We demonstrated that alloying of AlN with wurtzite structure and ScN with rock-salt structure results in enhancement of the PE properties of AlN - ScN composites. Thin films of ScN, AlN and $Al_{1-x}Sc_xN$ (x = 0 – 1.0) were prepared by dual co-sputtering and evaluated using x-ray diffraction, XPS, SEM, and PE characterization. In comparison to pure AlN thin films, up to 25% increase in PE coefficient for $Al_{1-x}Sc_xN$ (x = 0 – 0.7) thin films with wurtzite structure was observed. This augmentation of PE properties can be explained by the structural reorganization that occurs in the process of alloying of AlN with ScN.

The obtained results suggest that $Al_{1-x}Sc_xN$ films could be a promising novel PE material and has a prospective for further in-depth study and possible use in uncooled IR detectors.

REFERENCES

1. Y.-R. Wu, *IEEE Transactions*, **52** (2), 284 (2005).
2. V. Fufligin, E. Salley, A. Osinsky, and P. Norris, *Appl. Phys. Lett.* **77,** 3075 (2000).
3. E. Crisman, J. Derov, A. Drehman, at al., *J. Solid-State Lett.* **8** (3), H31 (2005).
4. E. Crisman, V. Vasilyev, A. Drehman, and R. Webster, *MRS Proceedings*, **1288** © 2011.
5. E. Crisman, A. Drehman, R. Miller, A. Osinsky, at al., *Phys. Stat. Sol. C* 11, 517 (2014).
6. G. Stan, M. Botea, G. Boni, I. Pintilie, and L. Pintilie, *Appl. Surf. Sci*. **353**, 1195 (2015).
7. H. Kim, B. Ju, Y. Lee, S. Lee, J. Lee, at al., *Sensors and Actuators A*. **89**, 255 (2001).
8. M. Akiyama, T. Kamohoara, K. Kano, A. Teshigahara, at al., *Adv. Mater*. **21**, 593 (2009).
9. M. Lee, R. Guo and A. Bhalla, *J. of Electroceramics.* **2(**4), 229 (1998).
10. F. Tasnádi, B. Alling, C. Höglund, at al., *Phys. Rev. Lett*., **104**, 137601 (2010).
11. R. Mozzi, G. Parry, G. Jeffrey, *J. of Chem. Phys.*, **23**, 406 (1955).
12. F. Moulder et al., Handbook of X-Ray Photoelectron Spectroscopy, Perkin-Elmer Co., Eden Prairie, MN (1992).
13. M. Daglish, *Integrated Ferroelectrics*, **22**, 473 (1998).
14. N. Farrer and L. Bellaiche, *Phys. Rev. B* **66**, 201203 (R) (2002).
15. C. Höglund, J. Birch, B. Alling, J. Bareńo, at al., *J. Appl. Phys*. **107**, 123515 (2010).
16. C. Höglund, J. Bareńo, J. Birch, B. Alling, at al., *J. Appl. Phys*. **105**, 113517 (2009).
17. H. Vollstädt, E. Ito, M. Akaishi, S. Akimoto, at al., *Proc. Japan. Acad. B*, **66**, 7 (1990).
18. R. Miller and A. Osinsky, *Agnitron Tech*., "Pyroelectric Properties of AlN Films", White Paper for AFRL (2013).
19. Yu. Shaldin and S. Matyjasik, *Semiconductors*. **45**(9), 1117 (2011).
20. S. Lang, Physics Today. **1**(8), 31 (2005).